

Search for Light CP-odd Higgs in Radiative Decays of $\Upsilon(1S)$

W. Love,¹ V. Savinov,¹ H. Mendez,² J. Y. Ge,³ D. H. Miller,³ I. P. J. Shipsey,³ B. Xin,³
 G. S. Adams,⁴ M. Anderson,⁴ J. P. Cummings,⁴ I. Danko,⁴ D. Hu,⁴ B. Moziak,⁴
 J. Napolitano,⁴ Q. He,⁵ J. Insler,⁵ H. Muramatsu,⁵ C. S. Park,⁵ E. H. Thorndike,⁵
 F. Yang,⁵ M. Artuso,⁶ S. Blusk,⁶ S. Khalil,⁶ J. Li,⁶ R. Mountain,⁶ S. Nisar,⁶
 K. Randrianarivony,⁶ N. Sultana,⁶ T. Skwarnicki,⁶ S. Stone,⁶ J. C. Wang,⁶ L. M. Zhang,⁶
 G. Bonvicini,⁷ D. Cinabro,⁷ M. Dubrovin,⁷ A. Lincoln,⁷ P. Naik,⁸ J. Rademacker,⁸
 D. M. Asner,⁹ K. W. Edwards,⁹ J. Reed,⁹ R. A. Briere,¹⁰ T. Ferguson,¹⁰ G. Tatishvili,¹⁰
 H. Vogel,¹⁰ M. E. Watkins,¹⁰ J. L. Rosner,¹¹ J. P. Alexander,¹² D. G. Cassel,¹²
 J. E. Duboscq,¹² R. Ehrlich,¹² L. Fields,¹² R. S. Galik,¹² L. Gibbons,¹² R. Gray,¹²
 S. W. Gray,¹² D. L. Hartill,¹² B. K. Heltsley,¹² D. Hertz,¹² J. M. Hunt,¹² J. Kandaswamy,¹²
 D. L. Kreinick,¹² V. E. Kuznetsov,¹² J. Ledoux,¹² H. Mahlke-Krüger,¹² D. Mohapatra,¹²
 P. U. E. Onyisi,¹² J. R. Patterson,¹² D. Peterson,¹² D. Riley,¹² A. Ryd,¹² A. J. Sadoff,¹²
 X. Shi,¹² S. Stroiney,¹² W. M. Sun,¹² T. Wilksen,¹² S. B. Athar,¹³ R. Patel,¹³ J. Yelton,¹³
 P. Rubin,¹⁴ B. I. Eisenstein,¹⁵ I. Karliner,¹⁵ S. Mehrabyan,¹⁵ N. Lowrey,¹⁵ M. Selen,¹⁵
 E. J. White,¹⁵ J. Wiss,¹⁵ R. E. Mitchell,¹⁶ M. R. Shepherd,¹⁶ D. Besson,¹⁷ T. K. Pedlar,¹⁸
 D. Cronin-Hennessy,¹⁹ K. Y. Gao,¹⁹ J. Hietala,¹⁹ Y. Kubota,¹⁹ T. Klein,¹⁹ B. W. Lang,¹⁹
 R. Poling,¹⁹ A. W. Scott,¹⁹ P. Zweber,¹⁹ S. Dobbs,²⁰ Z. Metreveli,²⁰ K. K. Seth,²⁰
 A. Tomaradze,²⁰ J. Libby,²¹ L. Martin,²¹ A. Powell,²¹ G. Wilkinson,²¹ and K. M. Ecklund²²

(CLEO Collaboration)

¹*University of Pittsburgh, Pittsburgh, Pennsylvania 15260, USA*

²*University of Puerto Rico, Mayaguez, Puerto Rico 00681*

³*Purdue University, West Lafayette, Indiana 47907, USA*

⁴*Rensselaer Polytechnic Institute, Troy, New York 12180, USA*

⁵*University of Rochester, Rochester, New York 14627, USA*

⁶*Syracuse University, Syracuse, New York 13244, USA*

⁷*Wayne State University, Detroit, Michigan 48202, USA*

⁸*University of Bristol, Bristol BS8 1TL, UK*

⁹*Carleton University, Ottawa, Ontario, Canada K1S 5B6*

¹⁰*Carnegie Mellon University, Pittsburgh, Pennsylvania 15213, USA*

¹¹*Enrico Fermi Institute, University of Chicago, Chicago, Illinois 60637, USA*

¹²*Cornell University, Ithaca, New York 14853, USA*

¹³*University of Florida, Gainesville, Florida 32611, USA*

¹⁴*George Mason University, Fairfax, Virginia 22030, USA*

¹⁵*University of Illinois, Urbana-Champaign, Illinois 61801, USA*

¹⁶*Indiana University, Bloomington, Indiana 47405, USA*

¹⁷*University of Kansas, Lawrence, Kansas 66045, USA*

¹⁸*Luther College, Decorah, Iowa 52101, USA*

¹⁹*University of Minnesota, Minneapolis, Minnesota 55455, USA*

²⁰*Northwestern University, Evanston, Illinois 60208, USA*

²¹*University of Oxford, Oxford OX1 3RH, UK*

²²*State University of New York at Buffalo, Buffalo, New York 14260, USA*

(Dated: July 9, 2008)

Abstract

We search for a non-SM-like CP-odd Higgs boson (a_1^0) with $m_{a_1^0} < 2m_b$ in radiative decays of the $\Upsilon(1S)$, using 21.5M $\Upsilon(1S)$ mesons directly produced in e^+e^- annihilation. We investigate $a_1^0 \rightarrow \tau^+\tau^-$ and $a_1^0 \rightarrow \mu^+\mu^-$ decay channels. No significant signal is found. We obtain upper limits on the product of $\mathcal{B}(\Upsilon(1S) \rightarrow \gamma a_1^0)$ and $\mathcal{B}(a_1^0 \rightarrow \tau^+\tau^-)$ or $\mathcal{B}(a_1^0 \rightarrow \mu^+\mu^-)$. Our $\tau^+\tau^-$ results are almost two orders of magnitude more stringent than previous upper limits. Our data provide no evidence for a Higgs state with a mass of 214 MeV decaying to $\mu^+\mu^-$. Existence of such a state was previously proposed as an explanation for 3 $\Sigma^+ \rightarrow p\mu^+\mu^-$ events, having $\mu^+\mu^-$ masses just above the kinematic threshold, observed by the HyperCP experiment. Our results constrain NMSSM models.

Direct searches at LEP for the Standard Model Higgs boson, a CP-even scalar, set a lower bound on its mass in excess of 10^2 GeV [1]. Many extensions of the Standard Model predict the existence of a CP-odd pseudoscalar Higgs boson (hereafter denoted as a_1^0), which could be light. For example, the Next-to-Minimal Super-Symmetric Model (NMSSM) with a_1^0 mass below the threshold for $a_1^0 \rightarrow b\bar{b}$ decay is particularly well motivated [2]. Radiative production in $\Upsilon(1S)$ decays, $\Upsilon(1S) \rightarrow \gamma a_1^0$, offers a unique experimental opportunity to search for such a state. The couplings of the Higgs to fermions are proportional to their masses, therefore enhanced with respect to lighter mesons. The expected rate is given by [3]:

$$\frac{\mathcal{B}(\Upsilon(1S) \rightarrow \gamma a_1^0)}{\mathcal{B}(\Upsilon(1S) \rightarrow \mu^+\mu^-)} = \frac{G_F m_b^2}{\sqrt{2}\pi\alpha} g_d^2 \left\{ 1 - \left(\frac{m_{a_1^0}}{m_{\Upsilon(1S)}} \right)^2 \right\} \mathcal{C},$$

where G_F is the Fermi constant, α is the fine structure constant, g_d is the a_1^0 coupling to the down-type fermions, and \mathcal{C} incorporates QCD and relativistic corrections. The coupling $g_d \propto \tan\beta \cos\theta_A$, where $\tan\beta$ is the ratio of vacuum expectations for the two Higgs doublets, and θ_A is the mixing angle between doublet and singlet CP-odd Higgs bosons (for $\theta_A = 90^\circ$, a_1^0 is a pure singlet and decouples from fermions); g_d depends on the detailed choice of SUSY parameters. For $m_{a_1^0} < 2m_b$, the decay $a_1^0 \rightarrow \tau^+\tau^-$ is expected to dominate, especially at large $\tan\beta$, $\mathcal{B}(a_1^0 \rightarrow \tau^+\tau^-) \sim 0.9$ [2]. For $m_{a_1^0} < 2m_\tau$, $a_1^0 \rightarrow \mu^+\mu^-$ decays are copious below the $s\bar{s}$ threshold. In fact, it has been suggested that 3 $\Sigma^+ \rightarrow p\mu^+\mu^-$ events observed by the HyperCP experiment [4] are due to a CP-odd Higgs with a mass of 214.3 ± 0.5 MeV [5].

The data for this search were acquired with the CLEO-III detector [6] operating at the Cornell Electron Storage Ring (CESR) and correspond to an integrated luminosity of 1.1 fb^{-1} at the $\Upsilon(1S)$, yielding $(21.5 \pm 0.4) \times 10^6$ resonant decays. We also use 7 fb^{-1} of data collected at and near the $\Upsilon(4S)$ resonance for continuum background studies.

The CLEO-III detector has a solid angle coverage of 93% of 4π for charged and neutral particles. The CsI calorimeter attains γ energy resolutions of about 2% for $E_\gamma \geq 1$ GeV and 5% at 100 MeV. The charged particle tracking system operated in a 1.5 T magnetic field along the beam axis and achieved a momentum (p) resolution of 0.35% at 1 GeV and a dE/dx resolution of 6%. The muon detector consists of the wire chambers located at 3, 5, and 7 hadronic interaction lengths (at normal incidence) of iron absorber.

We select events with exactly two tracks of opposite charge and at least one γ . The highest energy γ , which when paired with any other γ in the event, is not within three standard deviations (3σ) of the π^0 mass, is selected to be a candidate for $\Upsilon(1S) \rightarrow \gamma a_1^0$. Photons are defined as showers that do not match charged track projections into the calorimeter. For optimal energy resolution and smallest backgrounds the radiative-decay γ is required to be in the barrel part of the calorimeter ($|\cos\theta| < 0.8$). Its lateral shower profile must be consistent with an isolated electromagnetic shower. When applying the π^0 veto, we place loose requirements on the other (non-signal) photon. Namely, the other γ is not required to be isolated and the entire solid angle of the calorimeter is used for its detection. Its energy is required to be at least 30 MeV (60 MeV) in the barrel (endcap) part of the calorimeter. The π^0 veto suppresses $e^+e^- \rightarrow \tau^+\tau^-$, with at least one τ decaying to a channel with π^0 (mostly $\rho\nu$).

To select $a_1^0 \rightarrow \tau^+\tau^-$ candidates we require a missing energy between 2 and 7 GeV. The total energy calculation is based on charged track momenta (the pion mass is assumed) and calorimeter energy for the looser definition of the γ candidates (see above). To suppress hadronic events from the continuum production and $\Upsilon(1S)$ decays, at least one of the

charged tracks must be identified as an electron or a muon. Events with two electrons are discarded to suppress Bhabha like events. Besides being identified in the muon system, the μ candidate is required to have an energy deposited in the calorimeter (E) consistent with a minimum ionizing particle. The electron candidate must have E equal p within $\pm 15\%$. dE/dx consistency is required for leptons. The invariant mass of photons (except for the radiative-decay γ) plus the charged track not identified as a lepton is required to be less than 2 GeV. To suppress final state radiation, the cosine of the angle between any charged track and the γ candidate must be less than 0.99.

We search for evidence for a signal of a monochromatic peak in the γ energy distribution. Thus, our results assume that the a_1^0 natural width is negligible compared with the experimental resolution, an assumption which is expected to be true, with the exception of the heaviest masses probed in the $\tau^+\tau^-$ channel, due to possible mixing with the η_b [7]. CLEO previously published an alternative method for probing the a_1^0 mass approaching the $b\bar{b}$ states, which is not sensitive to assumptions about its width [8].

The selected event sample is composed mostly of continuum $e^+e^- \rightarrow (\gamma)\tau^+\tau^-$ events, where the γ candidate comes either from initial state radiation (ISR) or from a π^0 produced in τ decay, with the second γ not reconstructed. The background estimates are superimposed on top of the spectrum obtained at the $\Upsilon(1S)$ resonance in Fig. 1a. The continuum backgrounds are estimated by scaling the $\Upsilon(4S)$ distributions. There is also a significant contribution from $\Upsilon(1S) \rightarrow \tau^+\tau^-$ with the γ candidate coming from a π^0 decay. The observed γ spectrum with binning comparable to our γ energy resolution is shown in Fig. 1c. No significant peaks are observed.

The channel $a_1^0 \rightarrow \mu^+\mu^-$ is selected by identifying both muons. We require that the total observed energy be within 250 MeV of the center-of-mass energy. The invariant dimuon mass has better resolution than the γ energy, therefore we use it to look for the a_1^0 signal. The selected data are dominated by radiative μ -pairs with a hard radiative photon. The data selected at the peak of the $\Upsilon(1S)$ resonance are well described by scaling the data collected at and near the $\Upsilon(4S)$ as illustrated in Fig. 1b. The $\Upsilon(1S)$ distribution plotted with binning comparable to our dimuon mass resolution is shown in Fig. 1d. No significant peak is found except for the J/ψ produced by ISR.

The signal efficiency varies with Higgs mass, or equivalently, γ energy. In order to determine the efficiency, we generated signal Monte Carlo (MC) for several a_1^0 masses and interpolated for masses in between. Proper angular correlations were implemented in the MC for both the polar angle of the radiative γ and for τ polarizations [9]. The signal peaks observed in the dimuon mass (γ energy) distribution for $a_1^0 \rightarrow \mu^+\mu^-$ ($a_1^0 \rightarrow \tau^+\tau^-$) were fitted to a Gaussian (with an asymmetric low energy tail, i.e., a Crystal Ball line shape [10]) to determine reconstruction efficiency and detector resolution, which are shown in Fig. 2ac (bd). The fit to the $J/\psi \rightarrow \mu^+\mu^-$ ISR peak observed in the $\Upsilon(1S)$ data gives a value for the resolution consistent with the MC expectations for an $a_1^0 \rightarrow \mu^+\mu^-$ signal at that mass (Fig. 2d).

We have scanned the observed γ energy and dimuon mass distributions by fitting a signal peak on top of a cubic background polynomial, changing the peak position in steps equal to the detector resolution. The peak width was fixed to the MC expectations. The fit range was set to ± 0.5 of $\ln(E_\gamma)$ (± 0.25 of $\ln(M_{\mu\mu})$) around the peak position. The $J/\psi \rightarrow \mu^+\mu^-$ peak region was excluded within $\pm 3\sigma$, unless fitting a peak at the J/ψ mass. Since, in the dimuon channel, the continuum backgrounds saturate the $\Upsilon(1S)$ sample (see Fig. 1b), we simultaneously fit the background polynomial to the dimuon mass distribution obtained

from the higher statistics $\Upsilon(4S)$ data. The overall background normalization factor for the $\Upsilon(4S)$ data was included as a free parameter in the fit.

To test for possible bias in the fit procedure, we calculated average and root mean square (RMS) values of fitted signal amplitude (N) divided by its error (ΔN). In absence of any signal peaks, values of 0.0 and 1.0 are expected, respectively. The average value for the data is $+0.01 \pm 0.09$ (-0.06 ± 0.05) for the $\gamma\tau^+\tau^-$ ($\gamma\mu^+\mu^-$) sample, while the RMS is 1.16 ± 0.09 (1.05 ± 0.05). To cover the observed deviations from the expectations we assume 15% for a possible systematic error in the fit procedure.

The ratio of the fit likelihoods for a signal peak included in the fit (\mathcal{L}_{max}) and the data fit with the background term alone (\mathcal{L}_0) is used to calculate the peak significance in standard deviations, $\sqrt{2\ln(\mathcal{L}_{max}/\mathcal{L}_0)}$. No peak with significance above 3σ is found in the $\gamma\tau^+\tau^-$ data. In the $\gamma\mu^+\mu^-$ data, the ISR J/ψ peak has 8.3σ significance. There are two other mass points which produce peaks with significance slightly above 3σ : 3.3σ at 2041 ± 4 MeV and 3.1σ at 211.92 ± 0.15 MeV. For one trial, the probability (ϵ) of background fluctuations producing a peak with significance equal or larger to 3.3σ (3.1σ) is 0.05% (0.1%). We performed 482 fits to $\gamma\mu^+\mu^-$ spectrum with the peak positions separated by one unit of mass resolution. Assuming that peaks must be separated by at least 3 units of mass resolution to fluctuate independently, we performed about $n = 482/3 \approx 160$ statistically independent trials. The overall probability in our scan of producing at least one peak with significance of at least 3.3σ (3.1σ) is $1 - (1 - \epsilon)^n \approx 8\%$ (15%).

With no evidence for an a_1^0 signal we set upper limits on its possible production rate as a function of the a_1^0 mass. To determine upper limits on the signal event yield we fix the signal amplitude to positive values and minimize it with respect to the background parameters to obtain a likelihood for given signal amplitude. We then integrate the likelihood function and find a signal amplitude which bounds 90% of the total area. Dividing this event limit by efficiency and the number of $\Upsilon(1S)$ decays in our data we obtain upper limits on $\mathcal{B}(\Upsilon(1S) \rightarrow \gamma a_1^0) \times \mathcal{B}(a_1^0 \rightarrow l^+ l^-)$ ($l = \tau$ or μ), which are displayed in Fig. 3. The limits were scaled up by 20% to account for the possible systematic error in the fit procedure (15%), in the efficiency calculation (MC statistics, interpolation between MC points, detector modeling; together $< 10\%$), in number of $\Upsilon(1S)$ decays (2%), and in simulation of detector resolution (10%). Our upper limits on $\mathcal{B}(\Upsilon(1S) \rightarrow \gamma a_1^0) \times \mathcal{B}(a_1^0 \rightarrow \tau^+ \tau^-)$ are almost 2 orders of magnitude more stringent than previously obtained by ARGUS [11]. Our upper limits on $\mathcal{B}(\Upsilon(1S) \rightarrow \gamma a_1^0) \times \mathcal{B}(a_1^0 \rightarrow \mu^+ \mu^-)$ are the first experimental bounds.

Our $\gamma\tau^+\tau^-$ results provide stringent constraints on NMSSM models, eliminating a large portion of previously unconstrained parameter space. This is illustrated in Fig. 4, where NMSSM calculations by Dermisek, Gunion, McElrath [2] are compared to our upper limits. While some model parameters were fixed (e.g. $\tan\beta = 10$) in the theoretical calculations, other parameters were sampled. Each point represents a different choice of NMSSM parameter values consistent with the current experimental constraints. The plot on the right represents models with the additional requirement of low fine-tuning of electroweak symmetry breaking (see Ref.[2] for details). Color coding corresponds to various a_1^0 mass ranges. Our upper limits in various a_1^0 mass ranges are shown by horizontal lines. Solid (dashed) line(s) represent an average (minimal and maximal) upper limits in given mass range. Assuming that $\mathcal{B}(a_1^0 \rightarrow \tau^+ \tau^-)$ is 100%, the models above these lines are excluded. Our upper limits in the $\gamma\tau^+\tau^-$ channel for lower a_1^0 masses, $2m_\tau < m_{a_1^0} < 7.5$ GeV (red lines at the center of each plot), eliminate a significant fraction of models in this mass range (red points). Only very few models are challenged in the $7.5 < m_{a_1^0} < 8.8$ GeV range (green points and lines at

the sides of scatter plots). For higher masses (black points and lines touching the plot axes) our discriminating power fades away as the backgrounds increase while the expected signal rate decreases due to the phase space suppression. The non-singlet fraction of a_1^0 ($\cos\theta_A$) increases with falling $\tan\beta$ [2], though the net effect on g_d , and therefore $\mathcal{B}(\Upsilon(1S) \rightarrow \gamma a_1^0)$, is to decrease. At the same time, a_1^0 coupling to up-type fermions, $g_u \propto \cos\theta_A/\tan\beta$, increases, lowering $\mathcal{B}(a_1^0 \rightarrow \tau^+\tau^-)$. Thus, models with small $\tan\beta$ values are less constrained by our data.

Since $\mathcal{B}(a_1^0 \rightarrow \mu^+\mu^-)$ is not expected to be large above the $a_1^0 \rightarrow s\bar{s}$ threshold (~ 1 GeV), we did not transfer our limits on $\mathcal{B}(\Upsilon(1S) \rightarrow \gamma a_1^0)\mathcal{B}(a_1^0 \rightarrow \mu^+\mu^-)$ to Fig. 4, where NSSM model calculations of $\mathcal{B}(\Upsilon(1S) \rightarrow \gamma a_1^0)$ below the $\tau^+\tau^-$ threshold (blue points) were performed only for $m_{a_1^0} > 1$ GeV. Our limits below this mass value constrain NSSM scenarios. Of particular interest is our upper limit for $m_{a_1^0} = 214.3$ MeV, i.e., the $\mu^+\mu^-$ mass of $3\Sigma^+ \rightarrow p\mu^+\mu^-$ events observed by the HyperCP experiment [4]. The fit to our data (see Fig. 5) gives $7.0_{-4.5}^{+5.3}$ events at this mass and leads to an upper limit of $\mathcal{B}(\Upsilon(1S) \rightarrow \gamma a_1^0) < 2.3 \times 10^{-6}$ at 90% C.L. He, Tandean and Valencia showed that they could explain the HyperCP events with the a_1^0 hypothesis and still be consistent with the constraints from $K \rightarrow \pi\mu^+\mu^-$ experiments [5]. In their calculations they used $g_d^2 = 0.12$, while our upper limit translates into $g_d^2 < 0.026$ (using $\mathcal{C} = 0.5$ [3]), which calls for reevaluation of the a_1^0 hypothesis for the HyperCP events.

In summary, we have obtained meaningful upper limits on $\mathcal{B}(\Upsilon(1S) \rightarrow \gamma a_1^0) \times \mathcal{B}(a_1^0 \rightarrow \tau^+\tau^-)$ and $\mathcal{B}(\Upsilon(1S) \rightarrow \gamma a_1^0) \times \mathcal{B}(a_1^0 \rightarrow \mu^+\mu^-)$. Our limits on $\gamma\tau^+\tau^-$ are almost two orders of magnitude more stringent than those from ARGUS and eliminate a large portion of previously unconstrained parameter space in NMSSM models. Our limits on $\gamma\mu^+\mu^-$ challenge models with a_1^0 mass below $s\bar{s}$ threshold and the a_1^0 interpretation of HyperCP $3\Sigma^+ \rightarrow p\mu^+\mu^-$ events. Our limits are applicable to any light scalar or pseudo-scalar boson, which arises in various extensions of Standard Model.

We gratefully acknowledge the effort of the CESR staff in providing us with excellent luminosity and running conditions. This work was supported by the A.P. Sloan Foundation, the National Science Foundation, the U.S. Department of Energy, the Natural Sciences and Engineering Research Council of Canada, and the U.K. Science and Technology Facilities Council. We thank Radovan Dermisek, Jack Gunion, Michelangelo Mangano, German Valencia and Miquel Sanchis-Lozano for useful discussions of NMSSM models.

-
- [1] R. Barate *et al.*, Phys. Lett. B **565**, 61 (2003).
 - [2] R. Dermisek, J. F. Gunion and B. McElrath, Phys. Rev. D **76**, 051105(R) (2007).
 - [3] M. L. Mangano and P. Nason, Mod. Phys. Lett. A **22**, 1373 (2007), arXiv:0704.1719.
 - [4] H. Park *et al.* (HyperCP), Phys. Rev. Lett. **94**, 021801 (2005).
 - [5] X. G. He, J. Tandean and G. Valencia, Phys. Rev. Lett. **98**, 081802 (2007). The g_d coupling is denoted as l_d in this reference.
 - [6] Y. Kubota *et al.* (CLEO), Nucl. Instrum. Methods Phys. Res., A **320**, 66 (1992); D. Peterson *et al.*, *ibid.* A **478**, 142 (2002); M. Artuso *et al.*, *ibid.* A **554**, 147 (2005).
 - [7] E. Fullana and M. A. Sanchis-Lozano, Phys. Lett. B **653**, 67 (2007).
 - [8] D. Besson *et al.* (CLEO), Phys. Rev. Lett. **98**, 052002 (2007).
 - [9] Z. Was and M. Worek, Acta Phys. Polon. B **33**, 1875 (2002), arXiv:hep-ph/0202007.

- [10] T. Skwarnicki, Ph.D. Thesis, Cracow Institute of Nuclear Physics, DESY-F31-86-02, 1986.
- [11] H. Albrecht *et al.* (ARGUS), Phys. Lett. B **154** ,452 (1985).

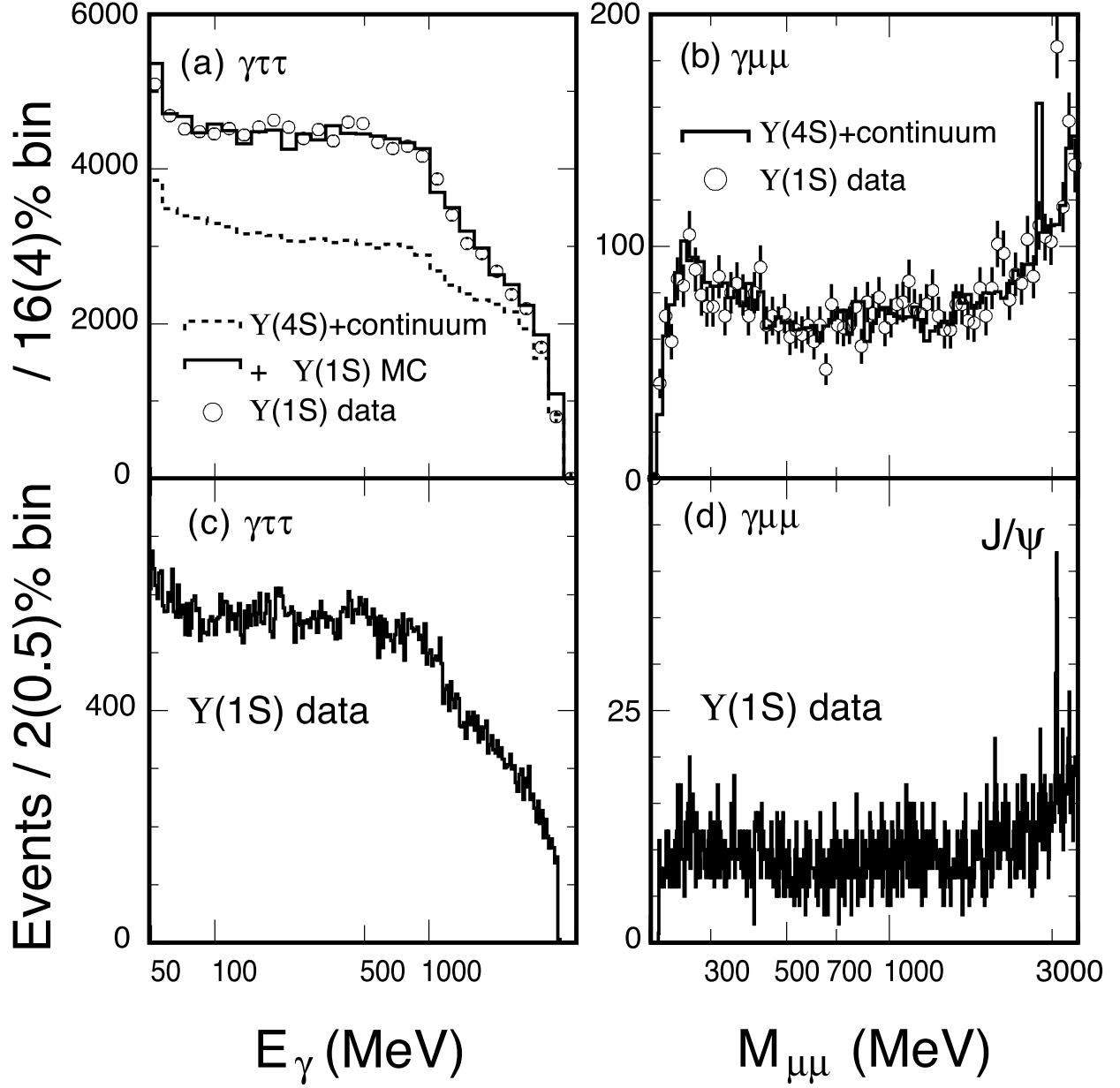


FIG. 1: Photon energy and dimuon mass distributions in $\gamma\tau^+\tau^-$ (a,c) and $\gamma\mu^+\mu^-$ (b,d) data, respectively. Bin size for the right column plots is given in the axes labels in parentheses. In the top row, the $\Upsilon(1S)$ data (points with error bars) are compared to the estimated backgrounds (dashed and solid lines). In the bottom row, the $\Upsilon(1S)$ data (solid line) are shown in fine binning comparable to the detector resolution (see bottom row of Fig. 2). In (b) the J/ψ ISR peak is shifted in the background estimate, since we scaled μ momenta down by the ratio of the beam energies when scaling the higher energy data to the $\Upsilon(1S)$ distribution.

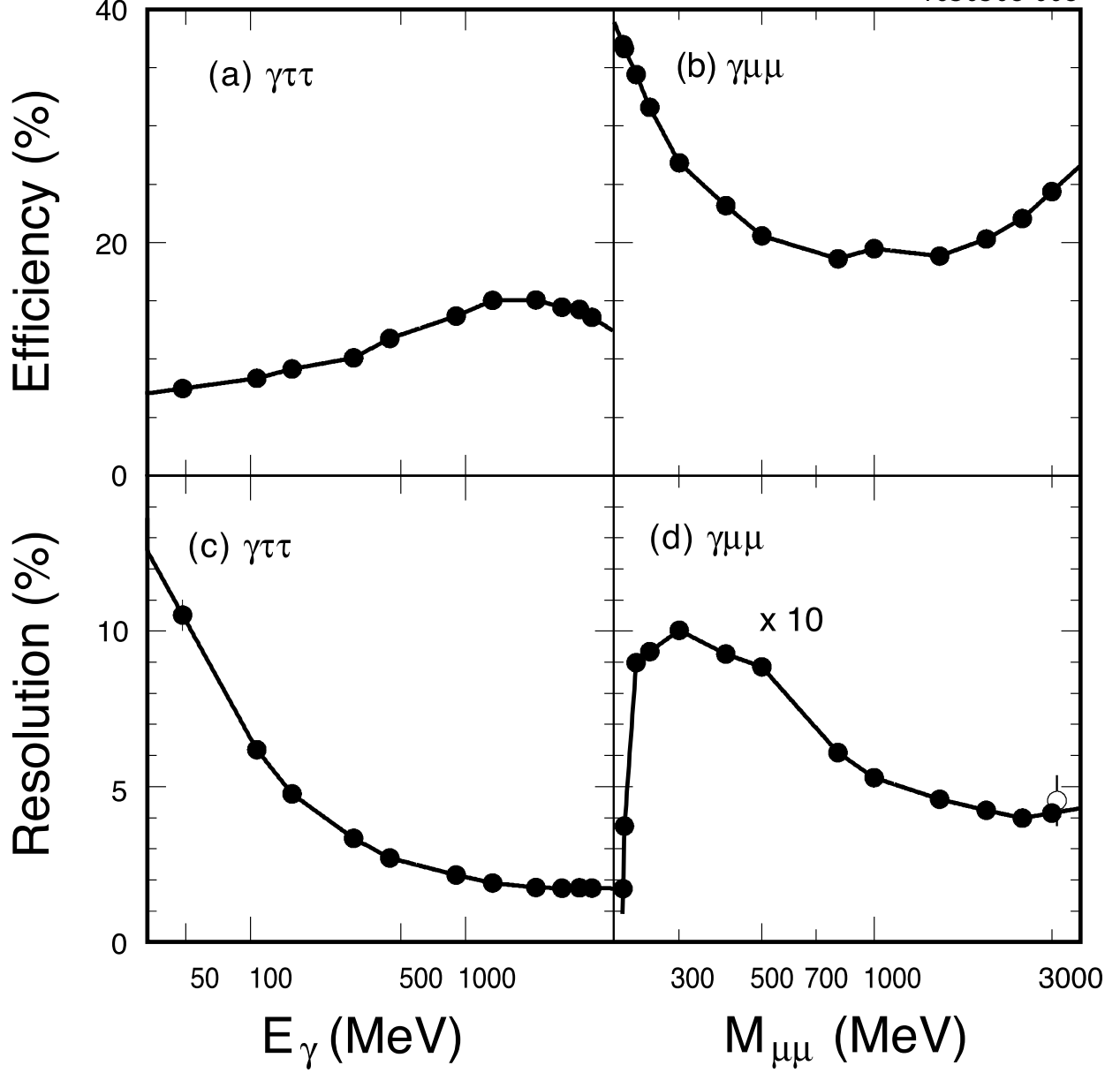


FIG. 2: Efficiency (a,b) and a_1^0 mass resolution (c,d) obtained from the fits to the $a_1^0 \rightarrow \tau^+\tau^-$ (left column) and $a_1^0 \rightarrow \mu^+\mu^-$ (right column) signal MC (points) and interpolated for the regions in between (solid line). In (d) relative dimuon mass resolution was multiplied by a factor of 10. See Appendix C of Ref. [3] for explanation of improvement of the dimuon mass resolution near the kinematic threshold. The hollow point with the error bar in (d) represents the fit of the mass resolution to the $J/\psi \rightarrow \mu^+\mu^-$ ISR peak observed in the $\Upsilon(1S)$ data.

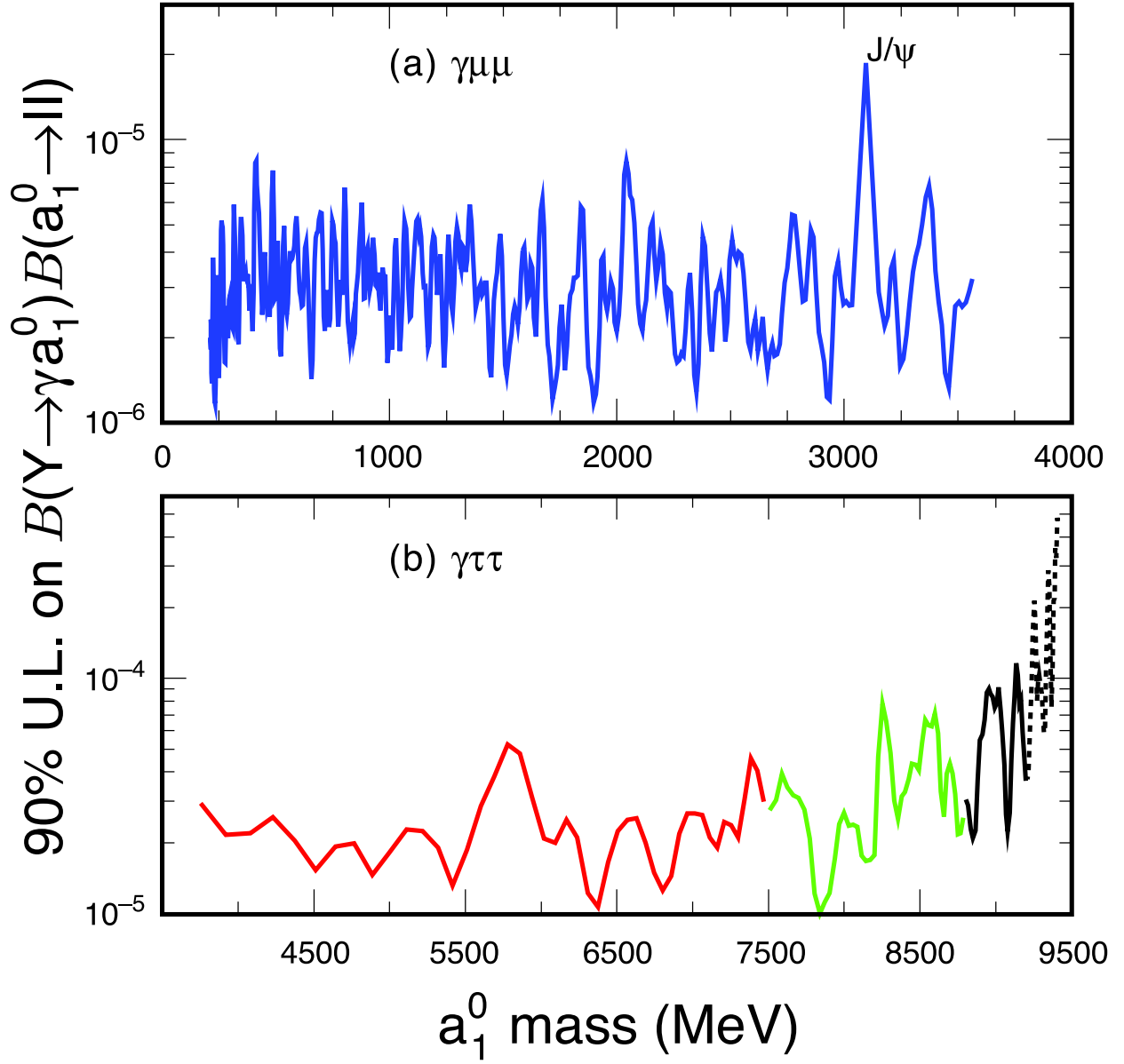


FIG. 3: Upper limits on $\mathcal{B}(\Upsilon(1S) \rightarrow \gamma a_1^0)$ (a) $\times \mathcal{B}(a_1^0 \rightarrow \mu^+ \mu^-)$ (b) $\times \mathcal{B}(a_1^0 \rightarrow \tau^+ \tau^-)$ as a function of the a_1^0 mass (90% C.L.). The color coding corresponds to the one used in Fig. 4. The dashed line indicates the region ($m_{a_1^0} > 9.2$ GeV) where a_1^0 is likely to mix with η_b and acquire a non-negligible width, thus invalidating our analysis method.

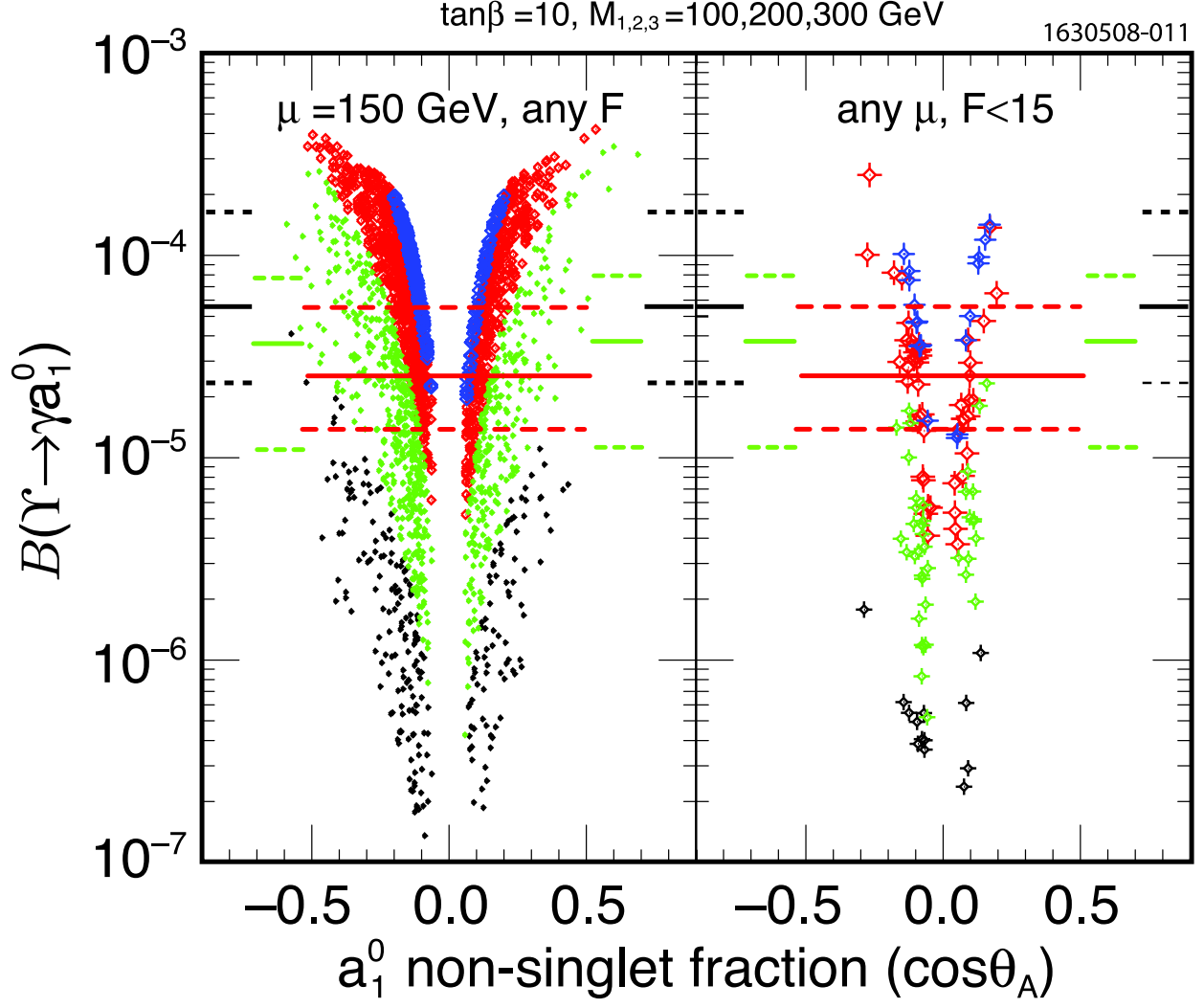


FIG. 4: Comparison of CLEO upper limits on $\mathcal{B}(\Upsilon(1S) \rightarrow \gamma a_1^0) \times \mathcal{B}(a_1^0 \rightarrow \tau^+ \tau^-)$ (solid and dashed lines) to the NMSSM predictions by Dermisek, Gunion, McElrath (points) [2]. See the text for explanations.

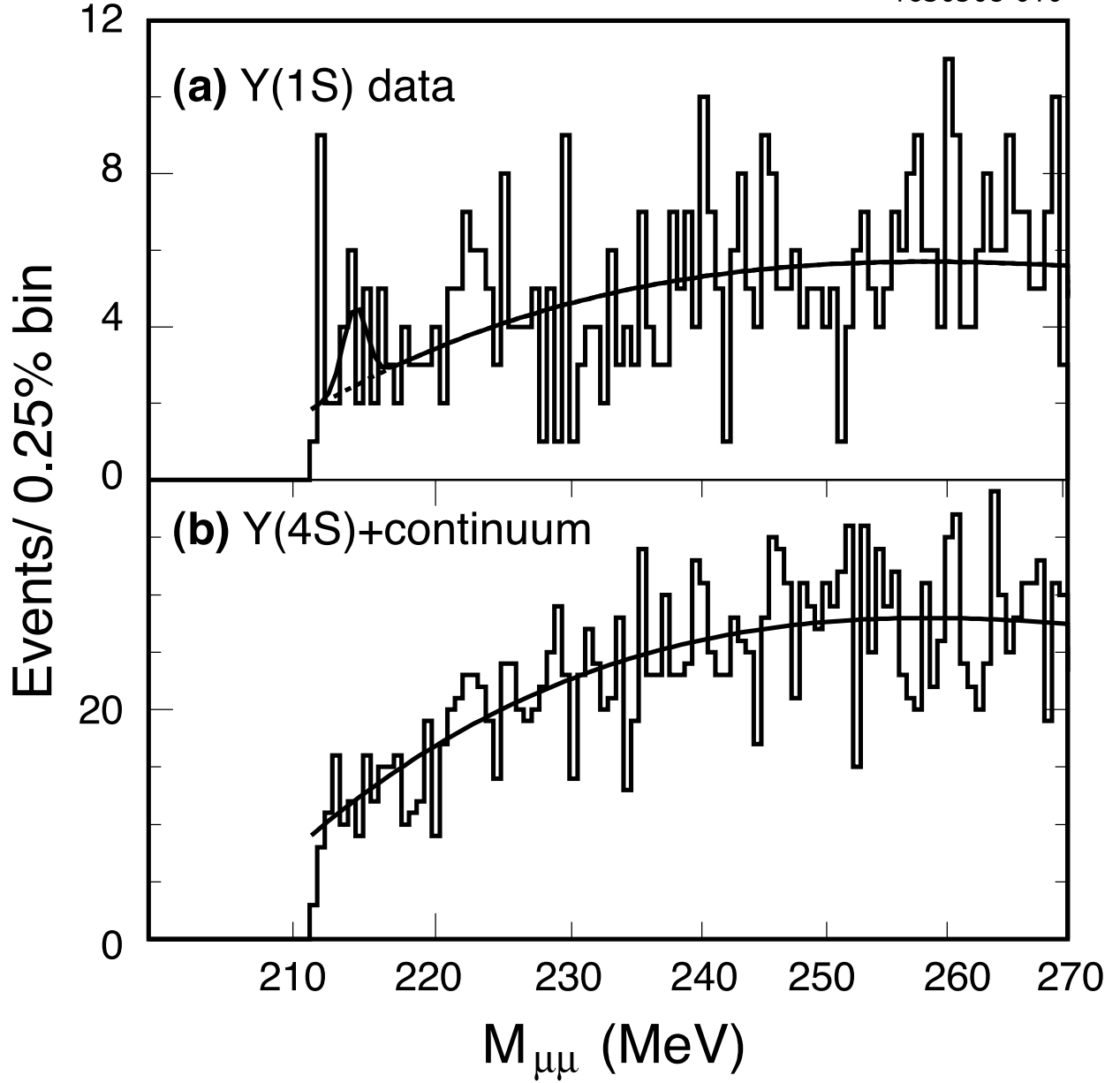


FIG. 5: A fit of a peak at a dimuon mass of 214.3 MeV with fixed width at the expected mass resolution, on top of cubic polynomial to our $\gamma\mu^+\mu^-$ data obtained at the $\Upsilon(1S)$ center-of-mass energy (a). The polynomial describing the continuum backgrounds was simultaneously constrained by the data collected at and near the $\Upsilon(4S)$ resonance (b).